PROCEEDINGS OF SCIENCE

Recent charm results from Belle

Longke Li*

On behalf of the Belle Collaboration
University of Cincinnati,
Cincinnati, Ohio 45221, U.S.

E-mail: lilk@ucmail.uc.edu

Recent charm results from Belle experiment are presented in this proceedings, including (1) measurement of mixing parameter $y_{CP} = (0.96 \pm 0.91 \pm 0.62^{+0.17}_{-0.00})\%$ in CP-odd decay for the first time, (2) the first Dalitz-plot analysis of $D^0 \to K^-\pi^+\eta$, (3) measurement of branching fractions of $\Lambda_c^+ \to \eta\Lambda^0\pi^+$ and $\eta\Sigma^0\pi^+$ and intermediate processes $\Lambda_c^+ \to [\Lambda(1670) \to \eta\Lambda^0]\pi^+$ and $\Lambda_c^+ \to \eta\Sigma(1385)^+$ relative to $\Lambda_c^+ \to pK^-\pi^+$: $0.293 \pm 0.003 \pm 0.014$, $0.120 \pm 0.006 \pm 0.006$, $(5.54 \pm 0.29 \pm 0.73) \times 10^{-2}$, and $0.192 \pm 0.006 \pm 0.016$, respectively, and (4) first determination of the spin and parity of a charmed-strange baryon $\Xi_c(2970)^+$ which is consistent with the HQSS prediction for $J^P(s_l) = 1/2^+(0)$.

40th International Conference on High Energy physics - ICHEP2020
July 28 - August 6, 2020
Prague, Czech Republic (virtual meeting)

*Speaker

https://pos.sissa.it/

PoS(ICHEP2020)391

1. Introduction to Belle at KEKB

KEKB [1] is an asymmetric-energy e^+e^- collider operating at and near $\Upsilon(4S)$ mass peak. As the only detector installed in KEKB, Belle detector has a good performance on momentum and vertex resolution, K/π separation etc. A detailed description of the Belle detector can be found elsewhere [2]. It has been ten years since the final full data set ($\sim$1 ab^{-1}) was accumulated, however, fruitful results on physics are lasting to be produced. Here we select some recent charm results from Belle to present in this proceedings.

2. Charm-mixing parameter y_{CP} in $D^0 \to K^0_S\omega$

The mixing parameter y_{CP} is measured in D^0 decays to the CP-odd final state $K^0_S\omega$ for the first time [3]. Considering mixing parameters $|x|$ and $|y| \ll 1$, the decay-time dependence of D^0 to a CP eigenstate is approximately exponential, $d\Gamma/dt \propto e^{-\Gamma(1+\eta_f y_{CP})t}$ where $\eta_f = +1$ (-1) for CP-even (-odd) decays. Along with the decay rate in flavored eigenstate decays $d\Gamma/dt \propto e^{-\Gamma t}$, the y_{CP} is determined by the decay proper-time value with the formula $y_{CP} = 1 - \frac{\tau(D^0\to K^-\pi^+)}{\tau(D^0\to K^0_S\omega)}$, where $D^0 \to K^-\pi^+$ is the chosen normalization mode with flavor eigenstate final state.

Based on the full Belle data sample of 976 fb^{-1}, we obtain 91 thousands of $D^0 \to K^0_S\omega$ and 1.4 millions of reference mode $D^0 \to K^-\pi^+$ in $M - \Delta M$ signal region, where M is the invariant mass of reconstructed D^0 and ΔM is the mass difference of reconstructed D^{*+} and D^0. Using unbinned maximum-likelihood fits for lifetime on these two samples with high purities, the proper decay-time of D^0 is determined as $\tau_{K^0_S\omega} = (410.47 \pm 3.73)$ fs and $\tau_{K\pi} = (406.53 \pm 0.57)$ fs, as shown in Fig. 1. Thus, we calculate $y_{CP} = (0.96 \pm 0.91 \pm 0.62^{+0.17}_{-0.00})\%$, where the first uncertainty is statistical, the second is systematic due to event selection and background, and the last is due to possible presence of CP-even decays in the data sample. This y_{CP} result is consistent with the world average value. In the future, comparing more precise measurements of y_{CP} with that of y may test the SM precisely or reveal new physics effects in the charm system.

3. Dalitz-plot analysis of $D^0 \to K^-\pi^+\eta$ decays

The understanding of hadronic charmed-meson decay is theoretically challenging due to the significant non-perturbative contributions, and input from experimental measurements thus plays an important role. A Dalitz-plot analysis of $D^0 \to K^-\pi^+\eta$ is performed for the first time at Belle based on 953 fb^{-1} of data [4]. Using a M-Q two-dimensional fit where M is the invariant-mass of reconstructed D^0 meson, $M = M(K^+\pi^-\eta)$, and Q is the released energy of D^{*+} decay, $Q = M(K^-\pi^+\eta\pi_s) - M - m_{\pi_s}$, a signal yield of 105 197 ± 990 is obtained in the signal region of 1.85 GeV$/c^2 < M <$ 1.88 GeV$/c^2$ and 5.35 MeV$/c^2 < Q <$ 6.35 MeV$/c^2$ with a high purity $(94.6 \pm 0.9)\%$. The Dalitz plot is well described by a combination of the six resonant decay channels $\bar{K}^*(892)^0\eta$, $K^-a_0(980)^+$, $K^-a_2(1320)^+$, $\bar{K}^*(1410)^0\eta$, $K^*(1680)^-\pi^+$ and $K^*_2(1980)^-\pi^+$, together with $K\pi$ and $K\eta$ S-wave components, as shown in Fig. 2. The dominant contributions to the decay amplitude arise from $\bar{K}^*(892)^0$, $a_0(980)^+$ and the $K\pi$ S-wave component. The $K\eta$ S-wave component, including $K^*_0(1430)^-$, is observed with a statistical significance of more than

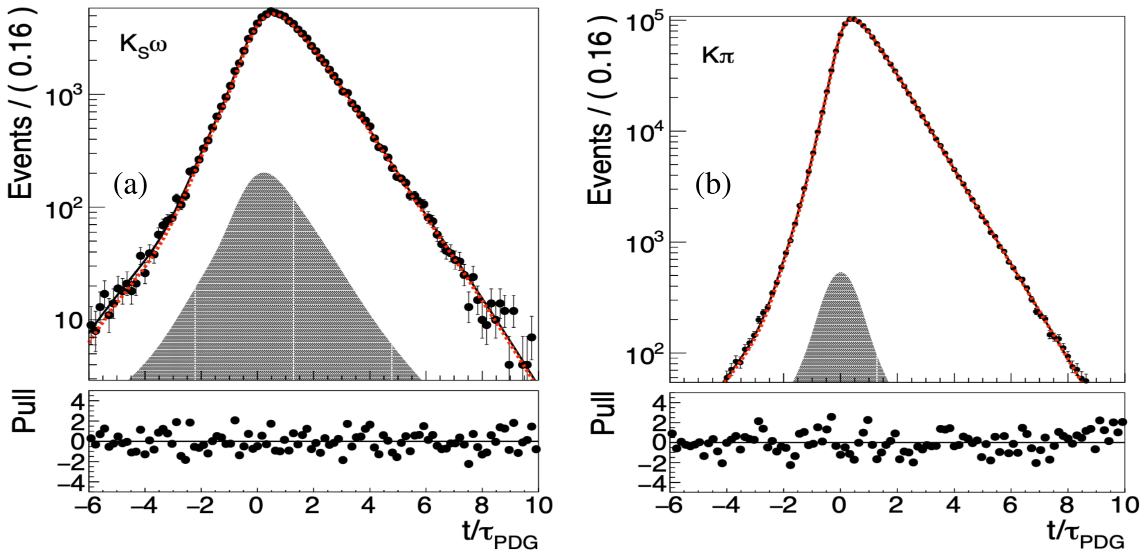

Figure 1: The fit of D^0 proper lifetime: (a) $D^0 \to K_S^0\omega$ and (b) $D^0 \to K^-\pi^+$. The dashed red curves are the signal contribution, and the shaded surfaces beneath are the background estimated from $M - \Delta M$ sidebands.

30σ, and the decays $K^*(1680)^- \to K^-\eta$ and $K_2^*(1980)^- \to K^-\eta$ are observed for the first time and have statistical significances of 16σ and 17σ, respectively.

We extract the signal yield from the D^0 invariant mass distribution in $1.78\ \mathrm{GeV}/c^2 < M < 1.94\ \mathrm{GeV}/c^2$ and $|Q - 5.85| < 1.0\ \mathrm{MeV}/c^2$, and obtain for the first time the branching ratio $\frac{\mathcal{B}(D^0\to K^-\pi^+\eta)}{\mathcal{B}(D^0\to K^-\pi^+)} = 0.500 \pm 0.002(\mathrm{stat}) \pm 0.020(\mathrm{syst}) \pm 0.003(\mathcal{B}_{\mathrm{PDG}})$, which corresponds to $\mathcal{B}(D^0 \to K^-\pi^+\eta) = (1.973 \pm 0.009(\mathrm{stat}) \pm 0.079(\mathrm{syst}) \pm 0.018(\mathcal{B}_{\mathrm{PDG}}))\%$. Then utilizing the world average branching fractions of intermediate resonant decays, the relative branching ratio $\frac{\mathcal{B}(K^*(1680)^-\to K^-\eta)}{\mathcal{B}(K^*(1680)^-\to K^-\pi^0)}$ is determined to be $0.11 \pm 0.02(\mathrm{stat})^{+0.06}_{-0.04}(\mathrm{syst}) \pm 0.04(\mathcal{B}_{\mathrm{PDG}})$. This is not consistent with the theoretical prediction under an assumption of a pure 1^3D_1 state [5]. We also determine the product of branching fraction $\mathcal{B}(D^0 \to [K_2^*(1980)^- \to K^-\eta]\pi^+) = (2.2^{+1.7}_{-1.9}) \times 10^{-4}$. For $a_0(980)^+$, we confirm the $\pi\eta'$ contribution in the three-channel Flatté model with a statistical significance of 10.1σ. We have also determined the branching fraction $\mathcal{B}(D^0 \to \bar{K}^*(892)^0\eta) = (1.41^{+0.13}_{-0.12})\%$, which is consistent with, and more precise than, the current world average of $(1.02 \pm 0.30)\%$. It deviates from the various theoretical predictions of (0.51-0.92)% [6] with a significance of more than 3σ.

4. Measurement of Branching Fractions of $\Lambda_c^+ \to \eta\Lambda\pi^+$, $\eta\Sigma^0\pi^+$, $\Lambda(1670)\pi^+$, and $\eta\Sigma(1385)^+$

The branching fractions of weakly decaying charmed baryons provide a way to study both strong and weak interactions. The $\Lambda_c^+ \to \eta\Lambda\pi^+$ decay mode is especially interesting since it has been suggested that it is an ideal decay mode to study the $\Lambda(1670)$ and $a_0(980)$ because, for any combination of two particles in the final state, the isospin is fixed. Based on a 980 fb^{-1} data sample, the branching fractions of $\Lambda_c^+ \to \eta\Lambda\pi^+$, $\eta\Sigma^0\pi^+$, $\Lambda(1670)\pi^+$, and $\eta\Sigma(1385)^+$ are measured [7]. The $M(\eta\Lambda\pi^+)$ spectrum is shown in Fig. 3 (a). The $\Lambda_c^+ \to \eta\Sigma^0\pi^+$ is observed indirectly as a feed-down component and it has efficiency-corrected yield $N_{cor} = (3.05 \pm 0.16) \times 10^5$. Considering

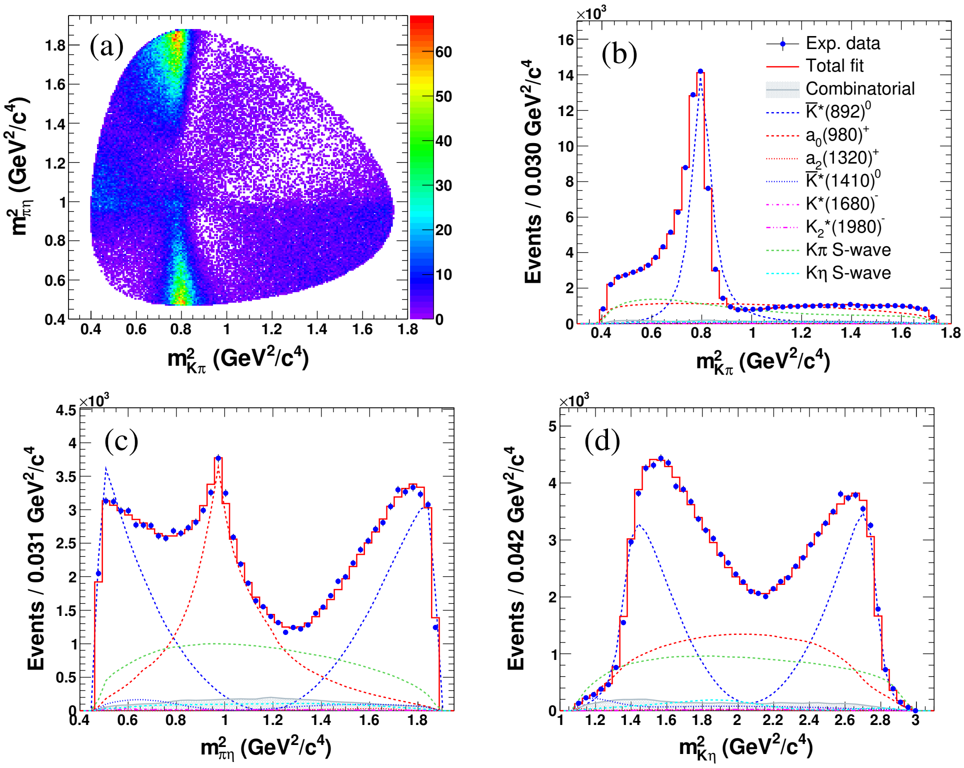

Figure 2: The Dalitz plot of $D^0 \to K^-\pi^+\eta$ in (a) M-Q signal region 1.85 GeV/c^2 $< M <$ 1.88 GeV/c^2 and 5.35 MeV/c^2 $< Q <$ 6.35 MeV/c^2, and projections on (b) $m^2_{K\pi}$, (c) $m^2_{\pi\eta}$ and (d) $m^2_{K\eta}$. In projections the fitted contributions of individual components are shown, along with contribution of combinatorial background (grey-filled) from sideband region.

$\Lambda_c^+ \to \eta\Lambda\pi^+$ and $\Lambda_c^+ \to pK^-\pi^+$ have sufficiently large statistic, the yields in individual bins of Dalitz plots are determined: $N_{cor}(\eta\Lambda\pi^+) = (7.41\pm0.07)\times10^5$ and $N_{cor}(pK^-\pi^+) = (1.005\pm0.001)\times10^7$. Finally, the branching ratios of $\Lambda_c^+ \to \eta\Lambda\pi^+$ and $\Lambda_c^+ \to \eta\Sigma^0\pi^+$ relative to $\Lambda_c^+ \to pK^-\pi^+$ are $0.293 \pm 0.003 \pm 0.014$ and $0.120 \pm 0.006 \pm 0.006$, where the uncertainties are statistical and systematic, respectively.

On the Dalitz plot of $\Lambda_c^+ \to \eta\Lambda\pi^+$ shown in Fig. 3 (b), bands corresponding to $\Lambda_c^+ \to \Lambda(1670)\pi^+/\eta\Sigma(1385)^+$ resonant sub-channels are seen clearly, along with $\Lambda_c^+ \to \Lambda a_0(980)^+$. For every 2 MeV/$c^2$ bin of $M(\eta\Lambda)$ and $M(\Lambda\pi^+)$ distributions, the Λ_c^+ yield is obtained by fitting $M(\eta\Lambda\pi^+)$. Then, a relativistic Breit-Wigner with momentum-dependent width is used to describe the S-wave $\Lambda(1670)$ and the P-wave $\Sigma(1385)$, as shown in Fig. 3 (c, d). Then, we determine the relative branching ratio $\frac{\mathcal{B}(\Lambda_c^+\to[\Lambda(1670)\to\eta\Lambda]\pi^+)}{\mathcal{B}(\Lambda_c^+\to pK^-\pi^+)} = (5.54 \pm 0.29 \pm 0.73)\%$ and $\frac{\mathcal{B}(\Lambda_c^+\to\eta\Sigma(1385)^+)}{\mathcal{B}(\Lambda_c^+\to pK^-\pi^+)} = 0.192 \pm 0.006 \pm 0.016$. Finally after using the world averaged $\mathcal{B}(\Lambda_c^+ \to pK^-\pi^+)$, we have $\mathcal{B}(\Lambda_c^+ \to [\Lambda(1670) \to \eta\Lambda]\pi^+) = (3.48 \pm 0.19 \pm 0.46 \pm 0.18) \times 10^{-3}$ and $\mathcal{B}(\Lambda_c^+ \to \eta\Sigma(1385)^+) = (1.21 \pm 0.04 \pm 0.10 \pm 0.06)\%$, where the first two uncertainties are statistical and systematic uncertainties, and the third uncertainty is from $\mathcal{B}(\Lambda_c^+ \to pK^-\pi^+)$.

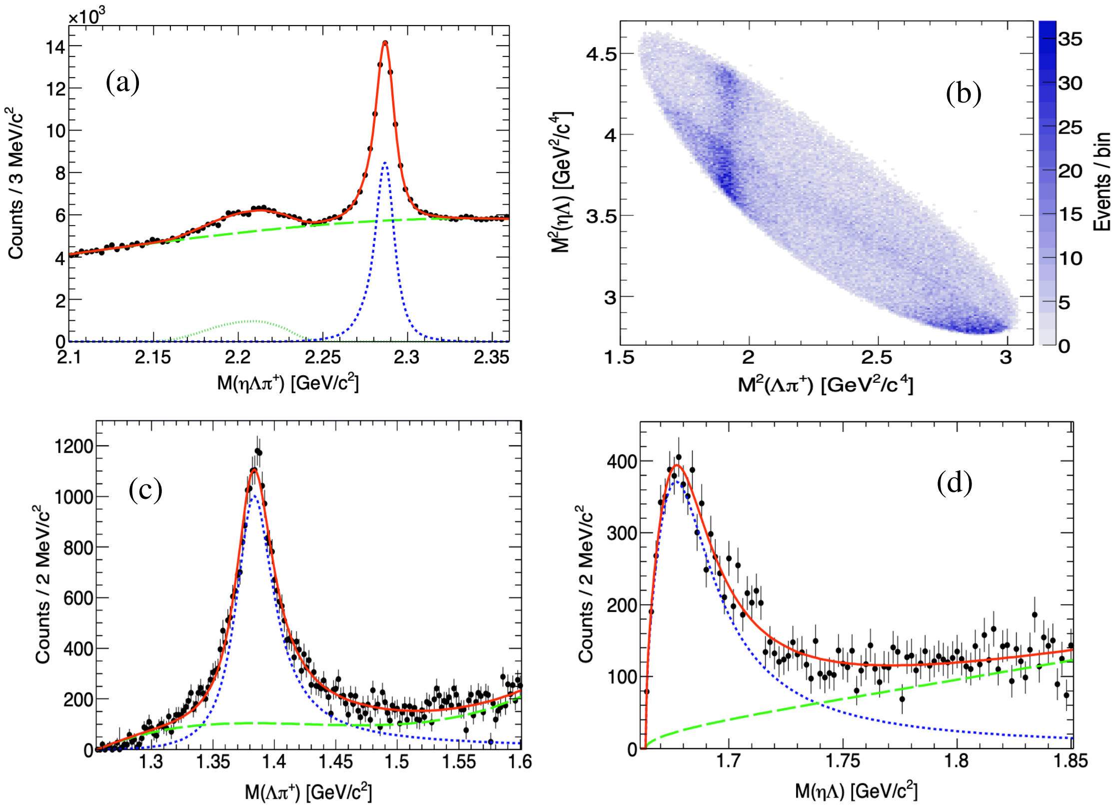

Figure 3: Top figures are (a) the invariant mass of $\eta\Lambda\pi^+$ and (b) its Dalitz plot in signal region. Bottom figures are fits to the Λ_c^+ yield in the (c) $M(\eta\Lambda)$ and (d) $M(\Lambda\pi^+)$ spectra, where the curves indicate the total fit result (solid red), the signal modeled with a relativistic Breit-Wigner function (dashed blue), and the background (long-dashed green).

5. First determination of the Spin and Parity of $\Xi_c(2970)^+$

The unclear theoretical situation motivates an experimental determination of spin and parity of a charmed-strange baryon $\Xi_c(2970)$, which provides important information to test predictions and help decipher its nature. Using a 980 fb^{-1} data sample, the spin and parity of a charmed-strange baryon $\Xi_c(2970)^+$ is measured [8] by (1) studies of the helicity angle distributions, θ_h of $\Xi_c(2970)^0$ and θ_c of $\Xi_c(2645)^0$ in $\Xi_c(2970)^+ \to \Xi_c(2645)^0\pi^+ \to \Xi_c^+\pi^-\pi^+$, and (2) a measurement of the $\Xi_c(2970)^+$ decay branching ratio $R = \mathcal{B}(\Xi_c(2970)^+ \to \Xi_c(2645)^0\pi^+)/\mathcal{B}(\Xi_c(2970)+ \to \Xi_c'^0\pi^+)$.

The angular distribution are obtained by dividing the data into 10 equal bins for $\cos\theta_h$ and $\cos\theta_c$, each within intervals of 0.2. The yield of $\Xi_c(2970)^+ \to \Xi_c(2645)^0\pi^+$ for each bin is obtained by fitting the invariant-mass distribution of $M(\Xi_c^+\pi^-\pi^+)$ for the $\Xi_c(2645)^0$ signal region (within 5 MeV/c^2 of $\Xi_c(2645)^0$ nominal mass) and sidebands (interval from 15 to 25 MeV/c^2 away from $\Xi_c(2645)^0$ nominal mass). The background-subtracted and efficiency-corrected yield distribution in Fig. 4 is fitted with expected decay-angle distributions W_J for different spin hypotheses. The best fit is for $J = 1/2$, while others are excluded with small significance, which shows inconclusive result. For helicity angle θ_c, with an assumption that the lowest partial wave dominates, the expected angular correlation $W(\theta_c)$ is used to describe the distribution. Finally the $J^P = 1/2^+$ hypothesis is better than $3/2^-$ or $5/2^+$ ones at the level of 5.1σ or 4.0σ.

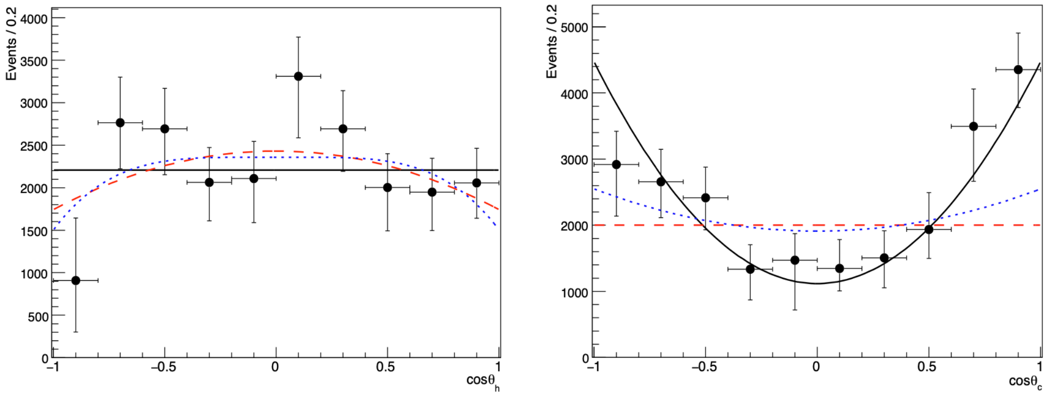

Figure 4: The yields on the cosine of helicity angle of $\Xi_c(2970)^0$ (left, $J = 1/2$ for solid black; $J = 3/2$ for dashed red; $J = 5/2$ for dotted blue) and on cosine of helicity angle of $\Xi_c(2645)^0$ (right, $J^P = 1/2^+$ for solid black; $J = 3/2^-$ for dashed red; $J = 5/2^+$ for dotted blue) in $\Xi_c(2970)^+ \to \Xi_c(2645)^0\pi^+$ decay.

The parity of $\Xi_c(2970)^+$ is established [8] from the ratio between $\mathcal{B}(\Xi_c(2970)^+ \to \Xi_c(2645)^0\pi^+)$ and $\mathcal{B}(\Xi_c(2970)^+ \to \Xi_c'^0\pi^+)$ by $R = \frac{N^*}{\epsilon^* N(\Xi_c^+)/\epsilon^+} / \frac{N'}{\sum_i \epsilon_i' N(\Xi_c^0)_i/\epsilon_i^0}$, where Ξ_c^0 uses two modes, $\Xi^-\pi^+$ and Ω^-K^+. The yields $N^{*,\prime}$ are obtained by fitting the invariant-mass distributions in Fig. 5. Finally we have $R = 1.67 \pm 0.29(stat)^{+0.15}_{-0.09}(syst) \pm 0.25(IS)$, where the last uncertainty is due to possible isospin-symmetry-breaking effects (15%). Heavy-quark spin symmetry (HQSS) predicts $R = 1.06$ (0.26) for a $1/2^+$ state with the spin of the light-quark degrees of freedom $s_l = 0$ (1) [9]. Our result favors a positive-parity assignment with $s_l = 0$. We note that HQSS predictions could be larger than the quoted value by a factor of ~ 2 with higher-order terms in $(1/m_c)$ [10], so our result is consistent with the HQSS prediction for $J^P(s_l) = 1/2^+(0)$.

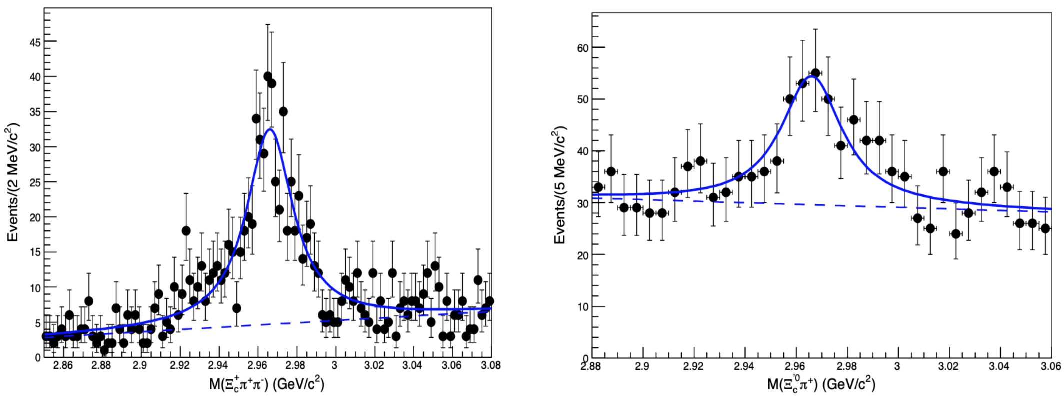

Figure 5: $\Xi_c^+\pi^-\pi^+$ invariant-mass distribution for $\Xi_c(2970)^+ \to \Xi_c(2645)^0\pi^+ \to \Xi_c^+\pi^-\pi^+$, and $\Xi_c'^0\pi^+$ invariant-mass distribution for $\Xi_c(2970)^+ \to \Xi_c'^0\pi^+ \to \Xi_c^0\gamma\pi^+$. The fit result (solid blue curve) is presented along with the background (dashed blue curve)

6. Summary

Belle experiment has achieved the fruitful productions of flavor physics to date. Some selected recent charm results are presented, including charm mixing parameter y_{CP} in CP-odd decay

$D^0 \to K_S^0\omega$, hadronic decays $D^0 \to K^-\pi^+\eta$ and $\Lambda_c^+ \to \eta\Lambda\pi^+/\eta\Sigma^0\pi^+$, first determination of the spin and parity of $\Xi_c(2970)^+$. More charming charm results from Belle will come out in near future. As a summary, I would like to say, "Belle is not only keeping alive but still keeping energetic, together with its upgraded experiment Belle II who is under a rapid growth."

References

[1] S. Kurokawa and E. Kikutani, Nucl. Instrum. Methods Phys. Res. Sect. A **499**, 1 (2003), and other papers included in this Volume.

[2] A. Abashian *et al.* (Belle Collaboration), Nucl. Instrum. Methods Phys. Res. Sect. A **479**, 117 (2002).

[3] M. Nayak *et al.* (Belle Collaboration), Phys. Rev. D **102**, 071102(R) (2020).

[4] Y. Q. Chen *et al.* (Belle Collaboration), Phys. Rev. D **102**, 012002 (2020).

[5] T. Barnes, N. Black, and P. R. Page, Phys. Rev. D **68**, 054014 (2003); C. Q. Pang, J. Z. Wang, X. Liu, *et al.* Eur. Phys. J. C (2017) 77: 861.

[6] H. Y. Cheng and C. W. Chiang, Phys. Rev. D **81**, 074021 (2010); H. N. Li, C. D. Lü, and F. S. Yu, Phys. Rev. D **86**, 036012 (2012); Q. Qin, H. N. Li, C. D. Lü, and F. S. Yu, Phys. Rev. D **89**, 054006 (2014).

[7] J. Y. Lee *et al.* (Belle Collaboration), arXiv:2008.11575.

[8] T. J. Moon *et al.* (Belle Collaboration), arXiv:2007.14700

[9] Hai-Yang Cheng and Chun-Khiang Chua, Phys. Rev. D **75**, 014006 (2007).

[10] Adam F. Falk and Thomas Mehen, Phys. Rev. D **53**, 231 (1996).